



**CytoMatrix for a reliable and simple characterization of lung
Cancer Stem Cells from Malignant Pleural Effusions**

Journal:	<i>Journal of Cellular Physiology</i>
Manuscript ID	JCP-19-1228.R1
Wiley - Manuscript type:	From the Bench
Date Submitted by the Author:	n/a
Complete List of Authors:	<p>Bruschini, Sara; Department of Experimental and Clinical Medicine, Magna Graecia University of Catanzaro, 88100 Catanzaro, Italy di Martino, Simona; IRCCS Regina Elena National Cancer Institute, 0128 Rome, Italy Pisanu, Maria Elena; High Resolution NMR Unit, Core Facilities, Istituto Superiore di Sanità, 00161 Rome, Italy Fattore, Luigi; Department of Clinical and Molecular Medicine, Sapienza University of Rome, Laboratory affiliated to Istituto Pasteur Italia-Fondazione Cenci Bolognetti De Vitis, Claudia; University of Rome "La Sapienza", Clinical and Molecular Medicine Laquintana, Valentina; IRCCS Regina Elena National Cancer Institute, 0128 Rome, Italy Buglioni, Simonetta; National Cancer Institute "Regina Elena", Department of Pathology Tabbi, Eugenio; University of Rome "La Sapienza", Clinical and Molecular Medicine Cerri, Andrea; IRCCS Regina Elena National Cancer Institute, 0128 Rome, Italy Visca, Paolo; IRCCS Regina Elena National Cancer Institute, 0128 Rome, Italy Alessandrini, Gabriele; IRCCS Regina Elena National Cancer Institute, 0128 Rome, Italy Facciolo, Francesco; IRCCS Regina Elena National Cancer Institute, 0128 Rome, Italy Napoli, Christian; Department of Medical Surgical Sciences and Translational Medicine, Sapienza University of Rome, 00189 Rome, Italy Trombetta, Marcella; Tissue Engineering and Chemistry for Engineering Lab, Department of Engineering, University Campus Bio-Medico, Rome, Italy Santoro, Antonio; UCS Diagnostic S.r.l. Rome, Italy Crescenzi, Anna; Section of Pathology, University Hospital Campus Bio-Medico of Rome, Rome, Italy Ciliberto, Gennaro; Istituto Regina Elena, Scientific Direction Mancini, Rita; University of Rome "La Sapienza", Clinical and Molecular Medicine</p>
Key Words:	NSCLC, CSCs, MPEs, CytoMatrix, SCD1

1
2
3
4
5
6
7
8
9
10
11
12
13
14
15
16
17
18
19
20
21
22
23
24
25
26
27
28
29
30
31
32
33
34
35
36
37
38
39
40
41
42
43
44
45
46
47
48
49
50
51
52
53
54
55
56
57
58
59
60



SCHOLARONE™
Manuscripts

CytoMatrix for a reliable and simple characterization of lung Cancer Stem Cells from Malignant Pleural Effusions

Sara Bruschini^{1°}, Simona di Martino^{2°}, Maria Elena Pisanu³, Luigi Fattore⁴, Claudia De Vitis⁵, Valentina Laquintana², Simonetta Buglioni², Eugenio Tabbi⁵, Andrea Cerri², Paolo Visca², Gabriele Alessandrini², Francesco Facciolo², Christian Napoli⁶, Marcella Trombetta⁷, Antonio Santoro⁸, Anna Crescenzi⁹, Gennaro Ciliberto^{10§}, Rita Mancini^{5§*}

¹Department of Experimental and Clinical Medicine, Magna Graecia University of Catanzaro, 88100 Catanzaro, Italy

²IRCCS Regina Elena National Cancer Institute, 0128 Rome, Italy

³High Resolution NMR Unit, Core Facilities, Istituto Superiore di Sanità, 00161 Rome, Italy

⁴Department of Clinical and Molecular Medicine, Sapienza University of Rome, Laboratory affiliated to Istituto Pasteur Italia-Fondazione Cenci Bolognetti

⁵Department of Clinical and Molecular Medicine, Sapienza University of Rome, 00161 Rome, Italy

⁶Department of Medical Surgical Sciences and Translational Medicine, Sapienza University of Rome, 00189 Rome, Italy

⁷Tissue Engineering and Chemistry for Engineering Lab, Department of Engineering, University Campus Bio-Medico, Rome, Italy

⁸UCS Diagnostic S.r.l. Rome, Italy

⁹Section of Pathology, University Hospital Campus Bio-Medico of Rome, Rome, Italy

¹⁰Scientific Directorate, IRCCS Regina Elena National Cancer Institute, 00128 Rome, Italy

[°]Co-first Authors: Authors contributed equally to this work

[§]Co-last Authors: Authors contributed equally to this work

*Corresponding Author: Rita Mancini, Department of Clinical and Molecular Medicine, Sapienza University of Rome, 00161 Rome, Italy Email: rita.mancini@uniroma1.it Phone Number: +39 0649766599 FAX number: +39 0649766599

Abstract

Cancer Stem cells (CSCs) are a subpopulation with the properties of extensive self-renewal, capability to generate differentiated cancer cells and resistance to therapies. We have previously shown that Malignant Pleural Effusions (MPEs) from patients with non-small cell lung cancer (NSCLC) represent a valuable source of cancer cells that can be grown as 3D spheroids enriched of stem-like features, which depend on the activation of the YAP-TAZ/Wnt- β catenin/SCD1 axis. Here, we describe a novel support, called CytoMatrix, for the characterization of limited amounts of cancer cells isolated from MPEs of patients with NSCLC. Our results show that this synthetic matrix allows an easy and fast characterization of several epithelial cellular markers. The use of CytoMatrix to study CSCs sub-populations confirms that SCD1 protein expression is enhanced in 3D spheroids as compared with 2D adherent cell cultures. YAP/TAZ nuclear-cytoplasmic distribution analyzed by CytoMatrix in 3D spheroids is highly heterogeneous and faithfully reproduces what observed in tumor biopsies. Our results confirm and extend the robustness of our workflow for the isolation and phenotypic characterization of primary cancer cells derived from lung MPEs and underscore the role of SCD1.

Keywords: Lung cancer, Cancer Stem Cells, MPEs, CytoMatrix, SCD1.

Abbreviations: NSCLC, Non-Small Cell Lung Cancer; CSCs, Cancer Stem Cells; MPEs, Malignant Pleural Effusions; SCD1, Stearoyl-CoA Desaturase 1; SFAs, Saturated Fatty Acids; MUFAs, Monounsaturated Fatty Acids; YAP, Yes-associated protein; TAZ, transcriptional coactivator with PDZ-binding motif; ICC, Immunocytochemistry; IHC, Immunohistochemistry; IF, Immunofluorescence; EGFR, Epidermal Growth Factor Receptor; ALK, Anaplastic Lymphoma Kinase; CTLA4, Cytotoxic T-Lymphocyte Antigen 4; PD-L1, Programmed Death-Ligand 1; ICI, Immune Checkpoint Inhibitor; ALDH, Aldehyde Dehydrogenases; EGF, Epidermal Growth Factor; bFGF, basic Fibroblast Growth Factor; TTF-1, Thyroid Transcription Factor-1; PAN-CK, Pan-Cytokeratin; CK7, Cytokeratin7; FISH, Fluorescent in Situ Hybridization; CDDP, Cisplatin; PEM, Pembrolizumab

1. INTRODUCTION

Lung cancer is the most common cause of cancer deaths. Approximately 85% of those cases are classified as non-small cell lung cancer (NSCLC) of which adenocarcinoma is the most common histological subtype. Despite advances in anti-cancer therapies the five-year survival rate (17.8%) for NSCLC is much lower than that of other leading cancers (Ettinger et al., 2017; Ferlay et al., 2015; Siegel, Miller, & Jemal, 2018).

For decades the gold standard therapy for NSCLC patients in the first line setting has been platinum-based doublet chemotherapy with targeted agents limited to subset of patients with specific genetic alterations such as EGFR mutations, or ALK and ROS translocations, and concomitant development of strategies for undruggable targets, such as KRAS mutations (Acunzo et al., 2017; Reck et al., 2014). The recent introduction of immunotherapy with checkpoint blockade inhibitors (ICI) directed against targets such as CTLA-4 and PD-1/PD-L1 is rapidly changing standard treatments for NSCLC patients as well as for several other advanced malignancies (Callahan, Postow, & Wolchok, 2016; Herbst et al., 2016; Reck et al., 2016). However, it is important to point out that the use of both cisplatin and ICI therapy results in an unfavourable outcome for a substantial proportion of patients due to drug resistance (Goss & Tsvetkova, ; Ilie et al., 2017).

A growing body of evidence suggests that treatment failures in patients with NSCLC can be attributed to the presence of a subpopulation of cancer cells with distinctive features, defined cancer stem cells (CSCs) (Lopez-Ayllon et al., 2014; Zhang et al., 2016). These cells are characterized by the ability to self-renew (Plaks, Kong, & Werb, 2015; Reya, Morrison, Clarke, & Weissman, 2001; Shackleton, Quintana, Fearon, & Morrison, 2009). CSCs, for their intrinsic stem like-properties, seem to be responsible for the development of resistance to anticancer treatments such as conventional chemotherapy, radiation and targeted therapies (Abdullah & Chow, 2013; Mihanfar et al., 2018; Pisanu et al., 2018; Yakisich, Azad, Kaushik, & Iyer, 2017). On the other hand, growing evidences suggest that CSCs are by themselves weakly immunogenic and are not efficiently recognized and eliminated by the immune system. In addition, CSCs have been postulated to foster the creation of an immune evading microenvironment, which is emerging as a critical element in limiting the efficacy of ICI therapy (Codd, Kanaseki, Torigo, & Tabi, 2018; Sultan et al., 2017).

One of the main difficulties consists in the isolation of CSCs, given their poor abundance in the tumour tissue, their slow replication kinetics, their plasticity and phenotypic heterogeneity (Grimshaw et al., 2008; Ricci-Vitiani et al., 2006). Even though several methods for isolating, propagating and characterizing CSCs have been developed (Collins, Berry, Hyde, Stower, &

1
2
3 Maitland, 2005; Eramo et al., 2007; Grimshaw et al., 2008; Hemmati et al., 2003; Ricci-Vitiani et
4 al., 2006), there is still the need to develop robust and reproducible protocols. In recent years we
5 and others have reported that malignant pleural effusions (MPEs) could represent an excellent
6 model to investigate tumour heterogeneity and to isolate putative CSCs, based on the rationale that
7 it is an easily accessible form of metastatic malignancy (Basak et al., 2009; Giarnieri et al., 2013;
8 Giarnieri et al., 2015; Mancini et al., 2011; Roscilli et al., 2016; Tiran et al., 2017). MPEs, defined
9 as pleural fluid containing malignant cells, are a complication caused by primary malignant pleural
10 mesothelioma or by metastatic cancers originating, most commonly, from lung and breast. MPEs
11 occurrence is observed in about 30% of lung cancer cases and is associated with poor prognosis
12 (Penz, Watt, Hergott, Rahman, & Psallidas, 2017). Among several techniques proposed to isolate
13 and enrich CSCs, many evidences support the concept that cell cultures in non-adherent conditions
14 and in a serum-free medium supplemented with growth factors promote the formation of spheroids
15 with stem-like properties (Eramo et al., 2007; Grimshaw et al., 2008; Mancini et al., 2011).

16
17 We previously reported a protocol to establish MPE-derived tumour cell cultures from NSCLC
18 patients. These cells can be grown in non-adherent conditions as 3D spheroids enriched for stem-
19 like properties, including upregulation of ALDH activity, Nanog, Oct4 and Sox2 markers, and give
20 rise efficiently to tumours, which reproduce the same histological features of the original human
21 tumour, when implanted in recipient mice (Mancini et al., 2011). Lung cancer 3D spheroids
22 overexpress genes involved in lipid metabolism. Among them we identified Stearoyl-CoA
23 desaturase 1 (SCD1), the main biosynthetic enzyme responsible for the conversion of saturated fatty
24 acids (SFAs) into monounsaturated fatty acids (MUFAs), as a key factor for lung CSCs and showed
25 that its inhibition reverts resistance to cisplatin treatment acting synergistically with chemotherapy
26 (Noto et al., 2013; Pisanu et al., 2017). At a mechanistic level SCD1 inhibition inactivates β -catenin
27 and YAP/TAZ signalling pathways, involved in the maintenance of the CSCs pool (Noto et al.,
28 2017). We also used primary MPE-derived tumour cultures as a tool for screening sensitivity to
29 chemotherapeutic agents and for genetic profiling, in order to select the most effective therapy
30 regimen (Roscilli et al., 2016).

31
32 Over the last five years we have been able to collect and analyse in our laboratory more than 300
33 MPE-derived NSCLC samples. Of these only approximately 15% are able to give rise to slowly
34 proliferating cultures that can be propagated for at least 4-5 passages. Primary cultures may be
35 difficult not only to establish, due to poor quality or abundance of biological material of origin, but
36 also to maintain for a sufficient number of passages to perform complex analyses (Janik et al.,
37 2016). Furthermore, MPEs contain a heterogeneous repertoire of cell types of which cancer cells
38 represent only a small fraction because they secrete cytokines and chemokines which promote the
39
40
41
42
43
44
45
46
47
48
49
50
51
52
53
54
55
56
57
58
59
60

1
2
3 recruitment of immunoregulatory cells, such as tumour-associated macrophages, that are the major
4 component of MPEs and are involved in cancer progression (L. Li et al., 2016). For all these
5 reasons it is important to subject MPE-derived cell cultures to a thorough phenotypic
6 characterization through the evaluation of a variety of markers. In order to avoid selection of
7 subpopulation of cells with particular growth advantages and which may not faithfully represent the
8 composition of the originating tumour, it is necessary to proceed to phenotypic characterization of
9 isolated cultures when the number of available cells is often very low (Janik et al., 2016). Hence,
10 there is a need to establish methods for the rapid characterization of cancer initiating cells soon after
11 their isolation. In this paper we describe the use of an innovative support, CytoMatrix, for the
12 characterization of limited amounts of cancer cells isolated from MPEs of patients with NSCLC.
13
14
15
16
17
18

20 21 **2. MATERIALS AND METHODS**

22 23 **2.1 MPEs samples processing and cell cultures**

24 Primary cell cultures were obtained from MPEs of patients (n = 2) with lung adenocarcinoma
25 enrolled by Istituti Fisioterapici Ospitalieri (IFO) under an Institutional Research Ethics Committee
26 approved protocol (N. 1032/17). All patients agreed to participate to the study and signed an
27 informed consent form, additional information regarding subjects' clinical history is reported in
28 Table 1. Tumor cells were isolated from MPEs as previously described (Mancini et al., 2011).
29 Briefly, pleural fluids (up to 1000 ml) were obtained by thoracentesis and collected aseptically in
30 non-heparinized bottles/tubes. After centrifugation at 1,200 rpm, for 5 min at 4°C, the supernatant is
31 decanted and the cell pellet resuspended in PBS. The procedure is repeated twice and then the cell
32 suspension layered on Oncoquick gradient (Greiner Bio One) to partially purify tumour cells from
33 the other MPEs components. Discontinuous gradient is then centrifuged at 800 g for 20 min at 4°C
34 with no brake. During the centrifugation step the cells are separated according to their different
35 buoyant densities: the denser fluid components such as erythrocytes and leucocytes migrate into the
36 lower phase through the bottom of the tube, **instead** the less dense cell fraction, including tumour
37 cells, is enriched at the interphase layer. After harvesting and washing step, tumour cells are
38 cultured in RPMI-1640 (Sigma, St. Louis, MO, USA) supplemented with 10 % FBS (Sigma, St.
39 Louis, MO, USA) to obtain 2D primary adherent cultures. 3D spheroids cultures were obtained
40 from adherent culture plating single cells at clonally density in ultra-low attachment flasks
41 (Corning, Corning, NY, USA) and in serum-free DMEM/F12 supplemented with bFGF (20ng/ml),
42 EGF (20ng/ml), insulin (20µg/ml), 0,5% glucose, heparin (5µg/ml) (Sigma, St. Louis, MO, USA),
43 B27 (Gibco, Invitrogen, Carlsbad, CA, USA).
44
45
46
47
48
49
50
51
52
53
54
55
56
57
58
59
60

1
2
3 Established human NSCLC cell line, NCI-H460, was obtained from ATCC (Manassas, VA, USA),
4 2D and 3D cultures were maintained as described for primary cells.

5
6 All cells were tested for mycoplasma contamination and subjected to Short Tandem Repeat (STR)
7 analysis by ATCC Cell Line Authentication Service (Manassas, VA, USA).
8
9

10 11 **2.2 Immunohistochemistry and immunocytochemistry**

12 Immunohistochemistry on formalin fixed paraffin-embedded tissue sections obtained from pleural
13 biopsy of human lung adenocarcinomas and immunocytochemistry on formalin fixed paraffin-
14 embedded cellular sections obtained from NCI-H460 cell line and MPES-primary cell lines
15 entrapped in CytoMatrix were performed on an automated immunostainer (Bond-III, Leica,
16 Biosystems, Italy). Briefly, paraffin sections were cut at 5µm using a microtome LEICA SM 2000R
17 (Advanced Research Systems Inc., Macungie, PA). The slides were dewaxed in xylene and
18 rehydrated through a series of graded ethanol solutions and stained with Gill's Hematoxylin (Bio-
19 optica, Milan) and Eosin (Bio-optica, Milan). A citrate buffer, pH 6 or pH 8 (for SCD1 and
20 YAP/TAZ staining), was used to unmask the antigens. The primary antibodies used are listed in
21 Table S1.
22
23

24 Images were obtained by using a light microscope (Microscope Nikon ECLIPSE 55i) equipped with
25 a Digital Image Capture software (Leica Application Suite V4.8).
26
27
28

29 30 31 32 33 **2.3 Immunofluorescence analysis and optical microscopy**

34 Immunofluorescence was performed on formalin fixed paraffin-embedded NCI-H460 cells
35 entrapped in CytoMatrix. After solvent dewaxing with Clearify Agent (Dako, Agilent, Santa Clara,
36 CA, USA) and antigen retrieval with a citrate buffer pH 8 in an automated immunostainer (Omnis,
37 Dako, Agilent, Santa Clara, CA, USA) immunofluorescence was performed as previously described
38 (Pisanu et al., 2018). Briefly, cells were fixed with 10% neutral buffered formalin, incubated 5 min
39 in glycine 0.1 M and permeabilized in 0.2 % Triton-X (Sigma-Aldrich, Milan, Italy). After washing
40 two times with PBS and blocking with 3% FBS in PBS the cells were stained with anti-YAP/TAZ
41 (Santa Cruz Biotechnologies, Dallas, Texas, USA) antibody (1:50 dilution) and incubated at 4 °C
42 overnight. Next day, cells were washed by PBS three times to remove unbound antibodies, then
43 secondary antibody (1:200 dilution) was added in the dark and incubated at room temperature for 1
44 h. Then cells were stained with Hoechst 33342 (1:1000 dilution) for 5 min in the dark.
45 Immunofluorescence images and morphology observations of cell lines were performed on
46 Axiocam Camera (Zeiss) digital camera coupled with Zeiss Axiovert optical microscope and
47 analyzed using ZEN core software (Zeiss).
48
49
50
51
52
53
54
55
56
57
58
59
60

2.4 Quantitative Real Time-PCR (qRT-PCR) analysis

For qRT-PCR total RNA was isolated by Trizol Reagent (Life Technologies, Gaithersburg, MD, USA) according to the manufacturer's guidelines. RNA was reverse-transcribed into cDNA using High Capacity RNA-to cDNA Kit (Applied Biosystems, Life Technologies, Gaithersburg, MD, USA). Quantitative RT-PCR was performed using SYBR green detection (Applied Biosystem, Life Technologies, Gaithersburg, MD, USA) and the $\Delta\Delta C_t$ method for relative quantification. Expression of Histone H3 or β -actin were used as internal control, as specified. The primers used for individual genes are listed in Table S2.

2.5 Sequencing Technologies

Formalin-fixed paraffin-embedded (FFPE) biopsy sections and primary cultures of tumour cells from MPEs of patient samples were processed by the Ion AmpliSeq Colon and Lung Cancer Panel (Life Technologies) and The Oncomine Focus Assay (Life Technologies).

For the Ion AmpliSeq Colon and Lung Cancer Panel DNA was extracted using the QIAamp DNA Mini Kit (Qiagen) according to the manufacturer's instructions. For library preparation 10 ng of DNA for each sample, obtained by using the Ion AmpliSeq Library 96LV Kit 2.0 (Life Technologies) and the Colon and Lung Cancer Panel (Life Technologies), were adopted. The panel provides 93 amplicons covering 504 mutational hotspot regions in 22 genes. The Ion Torrent Oncomine Focus Assay is a multi-biomarker next-generation sequencing (NGS) assay that permits immediate analysis of DNA and RNA to simultaneously detect multiple types of variants in 52 genes. In details it enables simultaneous detection of 35 targeted hotspot mutations, 23 fusion genes and 19 copy number variations (CNVs). A minimum of 10 ng of DNA and RNA were amplified using the NGS targeted panel Oncomine Focus Assay. On the Chef system (Life Technologies) was performed the template preparation by emulsion PCR (emPCR). In agreement with the manufacturer's instructions, library quality control was performed using the Ion Sphere Quality Control Kit in order to obtain that 10–30% of template positive Ion Sphere particles (ISP) were targeted in the emPCR reaction. At the end, sequencing primer and polymerase were added to the enriched ISPs and loaded onto Ion 520 (100 Mb output) chip. Each library was barcoded with the Ion Xpress Barcode Adapters 1–16 Kit (Life Technologies). Barcoded libraries were combined to a final concentration of 100 pM. Sequencing was performed on the Ion S5 (Life Technologies) platform. Data analysis was carried out with Torrent Suite Software V.3.2 (Life Technologies). The detected variants were annotated and filtered with the Ion Reporter software and reviewed with the Integrative Genomics Viewer v2.1 (Broad Institute, Cambridge, Massachusetts, USA). Nucleotide

1
2
3 variations detected by the Ion AmpliSeq Colon and Lung Cancer Panel and The OncoPrint Focus
4 Assay with less than a 5% variant frequency and covered by less than 1000 reads were not
5 considered. Fusion genes were considered positive when ≥ 20 fusion amplicons were found. CNVs
6 were annotated when confidence interval (CI) at 5% was ≥ 4 gene copies with ≤ 0.5 median of the
7 absolute value of all pairwise differences quality control measure.
8
9

10 11 12 **2.6 Statistical analysis**

13
14 All experiments were performed at least three times and values were calculated as mean \pm standard
15 deviation (SD) or standard error of the mean (SEM). Differences between two groups were
16 determined using Student's t-test and p values < 0.05 were considered statistically significant.
17
18

19 20 21 **3. RESULTS**

22 23 24 **3.1 CytoMatrix: a support to entrap limited amounts of cytological material from MPEs**

25
26 CytoMatrix is an innovative support originally designed to permit an easy and rational management
27 of the biological material from needle aspirates. A detailed study of different biocompatible
28 materials characterized by ion affinity for cell samples allowed to discover that chitosan derivatives
29 increase the effectiveness of the process of retaining cell suspensions dispensed on a synthetic
30 porous matrix. This study was conducted through a collaboration between the University Campus
31 Bio-Medico of Rome and the industrial partner UCS Diagnostic S.r.l., and led to the development,
32 and joint patenting of CytoMatrix (Pub No. WO2018083616, International Application No:
33 PCT/IB2017/056812). The powerful feature of this support is the ability to permit a rapid and
34 reliable diagnosis even in absence of large amounts of material. In line with this concept, we
35 thought that CytoMatrix could be a useful tool for the cytological evaluation of tumour cells
36 directly isolated from lung MPEs in order to obtain a rapid and complete phenotypic
37 characterization. CytoMatrix peculiarity is to efficiently restrain small amounts of biological
38 material inside its three-dimensional structure. The porous support is provided into a plastic bio-
39 cassette allowing to make easy the following steps of classical immunocytochemistry (ICC)
40 technique, such as formalin fixation, paraffin inclusion and microtome cut (Figure 1a).
41

42
43 Briefly, a minimum of 100,000 2D adherent cells that roughly correspond to 250 3D spheroids are
44 collected and centrifuged at 1,200 rpm for 5 min at 4°C. The supernatant is discarded and the cell
45 pellet is resuspended in 1mL of PBS and centrifuged at 1,200 rpm for 5 min at 4°C. After this
46 washing step the pellet is resuspended in a small volume of PBS (50-70 μ l) and a single drop of cell
47 suspension is laid on the matrix and trapped into its three-dimensional structure. Then the bio-
48
49
50
51
52
53
54
55
56
57
58
59
60

1
2
3 cassette is closed and processed according to a classical ICC protocol. The samples are formalin fixed,
4 blocked in paraffin, and the cellblock cut using a microtome into 5 μm sections, which are then
5 mounted onto slides. These slides are dewaxed in xylene and rehydrated through a series of graded
6 ethanol solutions and stained with Gill's Haematoxylin and Eosin, to assess the presence and the
7 morphology of the cells. Finally, the slides are subjected to unmasking process and incubation with
8 the primary antibodies in an automated immunostainer (see materials and methods). Starting from a
9 limited number of cells it is possible to obtain from each single CytoMatrix several slides to
10 perform a panel of immunostainings for various markers which result in an accurate characterization
11 of cells isolated from lung MPEs (Figure 1b).

12
13
14 In this context it is important to underline the possibility to exploit the biological material trapped
15 into CytoMatrix also to perform molecular analyses by extraction of DNA and RNA or other
16 investigations such as FISH and immunofluorescence and how a single tool permits to take
17 advantage of use a minimal amount of precious biological material to perform a reliable diagnosis
18 or research investigations also in the perspective of precision medicine.

27 **3.2 Characterization of primary cells from MPEs using CytoMatrix**

28
29 We first sought to set up the CytoMatrix-based immunostaining protocol using a stable lung cancer
30 cell line, namely NCI-H460, obtained from American Type Culture Collection (ATCC). Briefly,
31 NCI-H460 cells grown in 2D adherent conditions were harvested, resuspended in PBS and a drop of
32 cellular suspension was trapped into CytoMatrix before formalin fixation and paraffin inclusion.
33 Those samples were then evaluated for different markers by ICC. Our results, in line with ATCC
34 data, confirmed that NCI-H460 cells are characterized by a strongly positive immunostaining for
35 pan-cytokeratin (PAN-CK), a blend of cytokeratins (CKs), well-known epithelial cell markers.
36 Furthermore, those cells also presented positivity for vimentin, a mesenchymal marker that may be
37 co-expressed with CKs in a wide range of carcinomas. Of note, the pan leukocyte marker CD45 was
38 used as negative control (Figure 2a).

39
40
41 Thereafter, we decided to use CytoMatrix for the ICC characterization of primary cultures derived
42 from MPEs of patients with NSCLC. We describe here below the characterization of cell lines
43 isolated from MPEs of **three** representative cases with adenocarcinoma of the lung. Detailed
44 information regarding patients' clinicopathological history is provided in Table 1. To confirm the
45 epithelial origin of the isolated cells we performed a panel of immunostaining routinely used for
46 distinguishing lung adenocarcinoma cells: namely TTF-1, PAN-CK and CK7 (Carney, Kraynie, &
47 Roggli, 2015; Woo et al., 2017). Also, the pan leukocyte marker CD45 was evaluated to assess the
48 purity of cell preparations. As shown in **figure 2b** (and Figure S1) primary cells exhibited a marked

positivity for cytoplasmic PAN-CK and CK7 and a variable positivity for TTF-1 depending on cell line. As expected CD45 marker showed no staining in all the three cell lines. Finally, we compared CytoMatrix results with those obtained with standard immunohistochemistry (IHC) performed on the solid biopsy from the same patients (Figure 2b and supplementary Figure S1). We observed for all the three patients a complete correspondence of the results obtained with the two samples thus confirming the sensitivity of the CytoMatrix approach and also the maintenance in our culture conditions of the phenotypic features of the original tumour. Of note we have also observed a genotypic correspondence between pleural biopsy and low passage culture cells from the same patients, as showed by the analysis of mutational status reported in Table 1. It is important to point out that CytoMatrix also ensures the preservation of the cell morphology, tested by the routine Haematoxylin and Eosin staining (H&E).

Overall these results indicate that CytoMatrix constitutes a reliable support for the characterization with different cellular markers of primary cultures through ICC taking advantages of using minimum amount of precious biological material compared to classical approaches.

3.3 CytoMatrix for the study of MPEs-derived CSCs

Having documented the potential of CytoMatrix in the characterization of 2D adherent cell cultures established from MPEs of lung adenocarcinoma and given the evidences that MPEs represent an excellent model to isolate putative CSCs (Giarnieri et al., 2013; Mancini et al., 2011; Roscilli et al., 2016), we decided to evaluate if CytoMatrix was a useful tool for the study of this subpopulation of cells. To test this hypothesis, we first set the conditions to enrich the cell population with stem-like properties. When cultured in non-adherent conditions and in a serum-free medium supplemented with growth factors BBIRE-T238 and BBIRE-T248 MPE-derived primary cell lines were able to give rise to 3D spheroids at variable efficiency. On average 3D cultures were characterized by an enrichment of stem cell markers such as Nanog, Sox2 and Oct4. 3D spheroids from the stable lung cancer cell line, NCI-H460, previously characterized (Noto et al., 2013; Pisanu et al., 2017), were used as control (Figure 3a and b and supplementary Figure S2a and b).

3D primary spheroids were then subjected to the same phenotypic characterization performed on 2D adherent cells using CytoMatrix-based immunostaining. First, H&E counterstains showed the power of this tool to preserve the 3D structure of the spheroids. Moreover, when compared with either 2D adherent culture and the solid biopsy from the same patient the 3D spheroid culture showed the same pattern of expression, for the markers evaluated (Figure 3c and supplementary Figure S2c).

1
2
3 Recently, we and others have underlined the importance of lipid metabolism in controlling CSCs
4 maintenance (Igal, 2016; J. Li et al., 2017; Mancini et al., 2018). In line with previous studies where
5 we demonstrated that SCD1 is a key factor for the propagation of lung CSCs (Mancini et al., 2011;
6 Noto et al., 2013; Noto et al., 2017; Pisanu et al., 2017), we confirm here that 3D spheroids from
7 both the NCI-H460 NSCLC stable cell line and the BBIRE-T238 primary culture show increased
8 expression of SCD1 at mRNA level (Figure 3b). Furthermore, SCD1 expression was also assessed
9 by performing CytoMatrix ICC analyses. As shown in figure 3d SCD1 staining shows increased
10 expression of the protein in 3D spheroids compared with 2D adherent cell cultures. We also
11 observed that SCD1 staining on MPE-derived primary cultures is comparable to that obtained in the
12 solid biopsy from the same patient, confirming that cancer cells isolated from MPEs maintain in our
13 culture conditions the expression of SCD1 found in primary tumour (Figure 3d and supplementary
14 Figure S2d). When we performed the same evaluation on 3D vs 2D cultures from BBIRE-T248 we
15 did not observe upregulation in the expression of SCD1 at mRNA level (supplementary Figure S2b)
16 as well as at protein level (supplementary Figure S2d). This is, probably, due to patient
17 heterogeneity as also stated by a very recent evidence that some cancer cell lines may activate an
18 alternative fatty acid desaturation pathway to bypass the known pathway that is dependent on
19 SCD1 (Vriens et al., 2019).

20
21 SCD1 expression was previously shown by our group to correlate with YAP/TAZ nuclear
22 localization among different human lung adenocarcinoma samples (Noto et al., 2017). When we
23 evaluated the expression of YAP/TAZ in BBIRE-T238 and in BBIRE-T248 patient biopsies, we
24 observed that their subcellular localization is heterogeneous, and that only in some cells it is
25 possible to detect a strong nuclear localization (Figure 3e, upper panels and supplementary Figure
26 S2e, upper panels). As many evidences point to YAP/TAZ as key regulators of CSCs (Cordenonsi
27 et al., 2011; Hao et al., 2014; Hayashi et al., 2015) we used CytoMatrix immunostaining for their
28 evaluation in 3D primary spheroids. The staining reflects the result obtained from the patient's
29 biopsies, with some cells that maintain cytoplasmic localization and some with a strong nuclear
30 positivity, indicating that the 3D spheroid cell population is not homogeneous, and reflects the
31 heterogeneity found in the primary tumour (Figure 3e, lower panels and supplementary Figure S2e,
32 lower panels). Finally, we evaluated the YAP/TAZ localization also in 3D spheroids from the NCI-
33 H460 cell line by setting up a CytoMatrix Immunofluorescence (IF) staining. Slides obtained after
34 CytoMatrix processing were subjected to IF as described in materials and methods. The results
35 (Figure 3f) confirm also in this analysis a highly heterogeneous pattern of YAP/TAZ nuclear-
36 cytoplasmic localization. It has to be pointed out that Cytomatrix IF staining may suffer from
37
38
39
40
41
42
43
44
45
46
47
48
49
50
51
52
53
54
55
56
57
58
59
60

1
2
3
4
5
6
7
8
9
10
11
12
13
14
15
16
17
18
19
20
21
22
23
24
25
26
27
28
29
30
31
32
33
34
35
36
37
38
39
40
41
42
43
44
45
46
47
48
49
50
51
52
53
54
55
56
57
58
59
60

unspecific binding of secondary antibodies to the matrix and, therefore, deserves further optimization (not shown).

Overall these results underscore that CytoMatrix could be a useful tool not only for the phenotypic characterization of putative primary cancer cells isolated from lung MPEs but also for study of the key factors involved in the maintenance of stem-like properties in 3D spheroids.

4. DISCUSSION

In this paper we report on the use of CytoMatrix, a porous support for trapping minimal amounts of cells, that allows cell fixation, slice cutting and analysis by ICC and immunofluorescence. By presenting some examples of this procedure we show how CytoMatrix can easily allow the phenotypic characterization of small amounts of cancer cells derived from malignant pleural effusions and assess that our culture conditions allow to faithfully preserve the features of the original tumour. Moreover, we have also observed by NGS analysis, identical mutational patterns between a pleural biopsy and low passage culture cells from the same patients. CytoMatrix allows to generate from small amount of material, several slices, that can be subjected in theory to additional analyses such as electron microscopy, confocal microscopy, as well as DNA and RNA extraction for genomic studies.

Genomic analysis of CSC enriched 3D cultures from patients' samples coupled with drug testing may allow to set up a workflow to predict drug sensitivity of patients to new drug combinations, and to facilitate the application of new concepts of personalized medicine (Amirouchene-Angelozzi, Swanton, & Bardelli, 2017). In this respect the technology described in this report has the advantage to allow an excellent characterization of the effects of drug testing on phenotypic changes of lung CSCs entrapped in CytoMatrix and biomarker analysis and this can be in theory done in a rapid turnaround time of few days after CSCs isolation from malignant pleural effusions.

Gaining importance is being attributed to the possibility to reproduce *in vitro* the complexity of the tumour microenvironment through the establishment of tumour organoids (or tumoroids) where tumour cells are embedded within a tumour stroma and interact with cancer associated fibroblasts and cells of the innate and acquired immune system (Lee et al., 2018; Nadkarni, Abed, & Draper, 2016). Tumoroids are believed to allow a better study of immune-evasion mechanisms in cancer and to test in highly predictive systems the effect of immune-enhancing therapeutic approaches. However, one of the major limitations of tumoroids is the limited amount of biological material and their slow propagation in culture. In this regards the possibility to analyse in depth the structure of tumoroids embedded into CytoMatrix in normal conditions and after drug testing will open up new promising perspectives.

ACKNOWLEDGMENTS

This work was supported by Italian Association for Cancer Research (AIRC) grants IG15216 and IG19865 to G. Ciliberto and IG17009 to R. Mancini and by the LazioInnova grant 2018 n. 85-2017-13750 to R. Mancini.

We thank the inventors of CytoMatrix and the researchers of Cyto+ project: Federica Cascone, Daniele Nicoletti, Chiara Taffon, Pamela Mozetic, Marco Costantini, Alberto Rainer, Sara Maria Giannitelli. "Porous material for the inclusion of cytologic preparations, process for obtaining the same and its use". Pub No. WO2018083616. International Application No.: PCT/IB2017/056812. Publication Date: 2018 May 11.

<https://patentscope.wipo.int/search/en/detail.jsf?docId=WO2018083616&recNum=&maxRec=1000&office=&prevFilter=&sortOption=&queryString=&tab=PCTDescription>

"This work was supported by the project "Incremento del TRL della tecnologia CytoMatrix-Cyto+" funded in the framework of "INTESE: Innovazione e Trasferimento tecnologico per Sostenere la fruizione dei risultati della ricerca sul territorio" (prot. FILAS-RU-2014-1193, Lazio Region, Italy)". All the information regarding CytoMatrix acquisition and applications are available on the online website: <https://cytomatrix.it/>.

DATA AVAILABILITY STATEMENT

The data that support the findings of this study are available from the corresponding author upon reasonable request.

CONFLICT OF INTEREST

The authors declare no conflict of interest.

References

Abdullah, L. N., & Chow, E. K. (2013). Mechanisms of chemoresistance in cancer stem cells.

Clinical and Translational Medicine, 2(1), 3. doi:10.1186/2001-1326-2-3

- 1
2
3 Acunzo, M., Romano, G., Nigita, G., Veneziano, D., Fattore, L., Laganà, A., . . . Croce, C. M.
4
5 (2017). Selective targeting of point-mutated KRAS through artificial microRNAs. *Proc Natl*
6
7 *Acad Sci USA*, 114(21), E4203.
- 8
9 Amirouchene-Angelozzi, N., Swanton, C., & Bardelli, A. (2017). Tumor evolution as a therapeutic
10
11 target. *Cancer Discov*, 7(8), 805.
- 12
13 Basak, S. K., Veena, M. S., Oh, S., Huang, G., Srivatsan, E., Huang, M., . . . Batra, R. K. (2009).
14
15 The malignant pleural effusion as a model to investigate intratumoral heterogeneity in lung
16
17 cancer. *Plos One*, 4(6), e5884.
- 18
19 Callahan, M., Postow, M., & Wolchok, J. (2016). Targeting T cell co-receptors for cancer therapy.
20
21 *Immunity*, 44(5), 1069-1078. doi:10.1016/j.immuni.2016.04.023
- 22
23 Carney, J. M., Kraynie, A. M., & Roggli, V. L. (2015). Immunostaining in lung cancer for the
24
25 clinician. commonly used markers for differentiating primary and metastatic pulmonary
26
27 tumors. *Annals ATS*, 12(3), 429-435. doi:10.1513/AnnalsATS.201501-004FR
- 28
29 Codd, A. S., Kanaseki, T., Torigo, T., & Tabi, Z. (2018). Cancer stem cells as targets for
30
31 immunotherapy. *Immunology*, 153(3), 304-314. doi:10.1111/imm.12866
- 32
33 Collins, A. T., Berry, P. A., Hyde, C., Stower, M. J., & Maitland, N. J. (2005). Prospective
34
35 identification of tumorigenic prostate cancer stem cells. *Cancer Res*, 65(23), 10946.
- 36
37 Cordenonsi, M., Zanconato, F., Azzolin, L., Forcato, M., Rosato, A., Frasson, C., . . . Piccolo, S.
38
39 (2011). The hippo transducer TAZ confers cancer stem cell-related traits on breast cancer cells.
40
41 *Cell*, 147(4), 759-772. doi:<https://doi.org/10.1016/j.cell.2011.09.048>
- 42
43 Eramo, A., Lotti, F., Sette, G., Piloizzi, E., Biffoni, M., Di Virgilio, A., . . . De Maria, R. (2007).
44
45 Identification and expansion of the tumorigenic lung cancer stem cell population. *Cell Death*
46
47 *and Differentiation*, 15, 504.
- 48
49 Ettinger, D. S., Wood, D. E., Aisner, D. L., Akerley, W., Bauman, J., Chirieac, L. R., . . . Hughes,
50
51 M. (2017). **Non Small** cell lung cancer, version 5.2017, NCCN clinical practice guidelines in
52
53
54
55
56
57
58
59
60

- 1
2
3 oncology. *Journal of the National Comprehensive Cancer Network J Natl Compr Canc Netw*,
4
5 15(4), 504-535. doi:10.6004/jnccn.2017.0050
6
- 7 Ferlay, J., Soerjomataram, I., Dikshit, R., Eser, S., Mathers, C., Rebelo, M., . . . Bray, F. (2015).
8
9 Cancer incidence and mortality worldwide: Sources, methods and major patterns in
10
11 GLOBOCAN 2012. *International Journal of Cancer*, 136(5), E359-E386.
12
13 doi:10.1002/ijc.29210
14
- 15 Giarnieri, E., Bellipanni, G., Macaluso, M., Mancini, R., Holstein, A. C., Milanese, C., . . . Russo,
16
17 G. (2015). Review: Cell dynamics in malignant pleural effusions. *Journal of Cellular*
18
19 *Physiology*, 230(2), 272-277. doi:10.1002/jcp.24806
20
21
- 22 Giarnieri, E., De Vitis, C., Noto, A., Roscilli, G., Salerno, G., Mariotta, S., . . . Mancini, R. (2013).
23
24 EMT markers in lung adenocarcinoma pleural effusion spheroid cells. *Journal of Cellular*
25
26 *Physiology*, 228(8), 1720-1726. doi:10.1002/jcp.24300
27
28
- 29 Goss, G. D., & Tsvetkova, E. Drug resistance and its significance for treatment decisions in non-
30
31 small-cell lung cancer. *Current Oncology; Vol 19 (2012): Personalized Medicine in Metastatic*
32
33 *NSCLC: A Canadian Perspective* DO - 10.3747/Co.19.1113,
34
- 35 Grimshaw, M. J., Cooper, L., Papazisis, K., Coleman, J. A., Bohnenkamp, H. R., Chiapero-Stanke,
36
37 L., . . . Burchell, J. M. (2008). Mammosphere culture of metastatic breast cancer cells enriches
38
39 for tumorigenic breast cancer cells. *Breast Cancer Research*, 10(3), R52. doi:10.1186/bcr2106
40
41
- 42 Hao, J., Zhang, Y., Jing, D., Li, Y., Li, J., & Zhao, Z. (2014). Role of hippo signaling in cancer
43
44 stem cells. *Journal of Cellular Physiology*, 229(3), 266-270. doi:10.1002/jcp.24455
45
- 46 Hayashi, H., Higashi, T., Yokoyama, N., Kaida, T., Sakamoto, K., Fukushima, Y., . . . Baba, H.
47
48 (2015). An imbalance in TAZ and YAP expression in hepatocellular carcinoma confers cancer
49
50 stem cell-like behaviors contributing to disease progression. *Cancer Res*, 75(22), 4985.
51
52 doi:10.1158/0008-5472.CAN-15-0291
53
54
55
56
57
58
59
60

- 1
2
3 Hemmati, H. D., Nakano, I., Lazareff, J. A., Masterman-Smith, M., Geschwind, D. H., Bronner-
4 Fraser, M., & Kornblum, H. I. (2003). Cancerous stem cells can arise from pediatric brain
5 tumors. *Proc Natl Acad Sci USA*, *100*(25), 15178. doi:10.1073/pnas.2036535100
6
7
8
9 Herbst, R. S., Baas, P., Kim, D., Felip, E., Pérez-Gracia, J., L., Han, J., . . . Garon, E. B. (2016).
10 Pembrolizumab versus docetaxel for previously treated, PD-L1-positive, advanced non-small-
11 cell lung cancer (KEYNOTE-010): A randomised controlled trial. *The Lancet*, *387*(10027),
12 1540-1550. doi:10.1016/S0140-6736(15)01281-7
13
14
15
16
17 Igal, R. A. (2016). Stearoyl CoA desaturase-1: New insights into a central regulator of cancer
18 metabolism. *Biochimica Et Biophysica Acta (BBA) - Molecular and Cell Biology of Lipids*,
19 *1861*(12), 1865-1880. doi:<https://doi.org/10.1016/j.bbalip.2016.09.009>
20
21
22
23
24 Ilie, M., Benzaquen, J., Hofman, V., Lassalle, S., Yazbeck, N., Leroy, S., . . . C-H, M. a. (2017).
25 *Immunotherapy in non-small cell lung cancer: Biological principles and future opportunities*
26 doi:<http://dx.doi.org/10.2174/1566524018666180222114038>
27
28
29
30
31 Janik, K., Popeda, M., Peciak, J., Rosiak, K., Smolarz, M., Treda, C., . . . Ksiazkiewicz, M. (2016).
32 Efficient and simple approach to in vitro culture of primary epithelial cancer cells. *Bioscience*
33 *Reports*, *36*(6), e00423. doi:10.1042/BSR20160208
34
35
36
37 Lee, S. H., Hu, W., Matulay, J. T., Silva, M. V., Owczarek, T. B., Kim, K., . . . Shen, M. M. (2018).
38 Tumor evolution and drug response in patient-derived organoid models of bladder cancer. *Cell*,
39 *173*(2), 515-528.e17. doi:<https://doi.org/10.1016/j.cell.2018.03.017>
40
41
42
43
44 Li, J., Condello, S., Thomes-Pepin, J., Ma, X., Xia, Y., Hurley, T. D., . . . Cheng, J. (2017). Lipid
45 desaturation is a metabolic marker and therapeutic target of ovarian cancer stem cells. *Cell*
46 *Stem Cell*, *20*(3), 303-314.e5. doi:10.1016/j.stem.2016.11.004
47
48
49
50 Li, L., Yang, L., Wang, L., Wang, F., Zhang, Z., Li, J., . . . Zhang, Y. (2016). Impaired T cell
51 function in malignant pleural effusion is caused by TGF- β derived predominantly from
52 macrophages. *International Journal of Cancer*, *139*(10), 2261-2269. doi:10.1002/ijc.30289
53
54
55
56
57
58
59
60

- 1
2
3 Lopez-Ayllon, B., Moncho-Amor, V., Abarrategi, A., Ibañez, d. C., Castro-Carpeño, J., Belda-
4
5 Iniesta, C., . . . Sastre, L. (2014). Cancer stem cells and cisplatin-resistant cells isolated from
6
7 non-small-lung cancer cell lines constitute related cell populations. *Cancer Medicine*, 3(5),
8
9 1099-1111. doi:10.1002/cam4.291
10
- 11 Mancini, R., Giarnieri, E., De Vitis, C., Malanga, D., Roscilli, G., Noto, A., . . . Ciliberto, G.
12
13 (2011). Spheres derived from lung adenocarcinoma pleural effusions: Molecular
14
15 characterization and tumor engraftment. *PloS One*, 6(7), e21320; e21320-e21320.
16
17 doi:10.1371/journal.pone.0021320
18
- 19 Mancini, R., Noto, A., Pisanu, M. E., De Vitis, C., Maugeri-Saccà , M., & Ciliberto, G. (2018).
20
21 Metabolic features of cancer stem cells: The emerging role of lipid metabolism. *Oncogene*,
22
23 37(18), 2367-2378. doi:10.1038/s41388-018-0141-3
24
25
- 26 Mihanfar, A., Aghazadeh Attari, J., Mohebbi, I., Majidinia, M., Kaviani, M., Yousefi, M., &
27
28 Yousefi, B. (2018). Ovarian cancer stem cell: A potential therapeutic target for overcoming
29
30 multidrug resistance. *Journal of Cellular Physiology*, 0(0) doi:10.1002/jcp.26768
31
32
- 33 Nadkarni, R. R., Abed, S., & Draper, J. S. (2016). Organoids as a model system for studying human
34
35 lung development and disease. *Biochemical and Biophysical Research Communications*;
36
37 *Special Issue: Stem Cells*, 473(3), 675-682. doi:<https://doi.org/10.1016/j.bbrc.2015.12.091>
38
- 39 Noto, A., de Vitis, C., Pisanu, M. E., Roscilli, G., Ricci, G., Catizone, A., . . . Mancini, R. (2017).
40
41 Stearoyl-CoA-desaturase 1 regulates lung cancer stemness via stabilization and nuclear
42
43 localization of YAP/TAZ. *Oncogene*, doi:10.1038/onc.2017.75
44
45
- 46 Noto, A., Raffa, S., De Vitis, C., Roscilli, G., Malpicci, D., Coluccia, P., . . . Mancini, R. (2013).
47
48 Stearoyl-CoA desaturase-1 is a key factor for lung cancer-initiating cells. *Cell Death &*
49
50 *Disease*, 4(12), e947-e947. doi:10.1038/cddis.2013.444
51
- 52 Penz, E., Watt, K. N., Hergott, C. A., Rahman, N. M., & Psallidas, I. (2017). Management of
53
54 malignant pleural effusion: Challenges and solutions. *Cancer Management and Research*, 9,
55
56 229-241. doi:10.2147/CMAR.S95663
57
58
59
60

- 1
2
3 Pisanu, M. E., Noto, A., De Vitis, C., Morrone, S., Scognamiglio, G., Botti, G., . . . Mancini, R.
4
5 (2017). Blockade of stearyl-CoA-desaturase 1 activity reverts resistance to cisplatin in lung
6
7 cancer stem cells. *Cancer Letters*, 406, 93-104. doi:S0304-3835(17)30463-9 [pii]
8
- 9 Pisanu, M. E., Maugeri-Saccà, M., Fattore, L., Bruschini, S., De Vitis, C., Tabbi, E., . . . Mancini,
10
11 R. (2018). Inhibition of stearyl-CoA desaturase 1 reverts BRAF and MEK inhibition-induced
12
13 selection of cancer stem cells in BRAF-mutated melanoma. *Journal of Experimental &*
14
15 *Clinical Cancer Research*, 37(1), 318. doi:10.1186/s13046-018-0989-7
16
17
- 18 Plaks, V., Kong, N., & Werb, Z. (2015). The cancer stem cell niche: How essential is the niche in
19
20 regulating stemness of tumor cells? *Cell Stem Cell*, 16(3), 225-238.
21
22 doi:10.1016/j.stem.2015.02.015
23
- 24 Reck, M., on behalf of the ESMO Guidelines, Working Group, Popat, S., on behalf of the ESMO
25
26 Guidelines, Working Group, Reinmuth, N., on behalf of the ESMO Guidelines, Working Group,
27
28 . . . on behalf of the ESMO Guidelines, Working Group. (2014). Metastatic non-small-cell lung
29
30 cancer (NSCLC): ESMO clinical practice guidelines for diagnosis, treatment and follow-up.
31
32 *Annals of Oncology*, 25, iii27-iii39.
33
34
- 35 Reck, M., Rodríguez-Abreu, D., Robinson, A. G., Hui, R., Csósz, T., Fülöp, A., . . . Brahmer, J. R.
36
37 (2016). Pembrolizumab versus chemotherapy for PD-L1 Positive Non Small-Cell lung cancer.
38
39 *N Engl J Med*, 375(19), 1823-1833. doi:10.1056/NEJMoa1606774
40
- 41 Reya, T., Morrison, S. J., Clarke, M. F., & Weissman, I. L. (2001). Stem cells, cancer, and cancer
42
43 stem cells. *Nature*, 414, 105.
44
45
- 46 Ricci-Vitiani, L., Lombardi, D. G., Pilozzi, E., Biffoni, M., Todaro, M., Peschle, C., & De Maria, R.
47
48 (2006). Identification and expansion of human colon-cancer-initiating cells. *Nature*, 445, 111.
49
- 50 Roscilli, G., De Vitis, C., Ferrara, F. F., Noto, A., Cherubini, E., Ricci, A., . . . Mancini, R. (2016).
51
52 Human lung adenocarcinoma cell cultures derived from malignant pleural effusions as model
53
54 system to predict patients chemosensitivity. *Journal of Translational Medicine*, 14(1)
55
56 doi:10.1186/s12967-016-0816-x
57
58
59
60

- 1
2
3 Shackleton, M., Quintana, E., Fearon, E. R., & Morrison, S. J. (2009). Heterogeneity in cancer:
4
5 Cancer stem cells versus clonal evolution. *Cell*, *138*(5), 822-829.
6
7 doi:10.1016/j.cell.2009.08.017
8
- 9 Siegel, R. L., Miller, K. D., & Jemal, A. (2018). Cancer statistics, 2018. *CA: A Cancer Journal for*
10
11 *Clinicians*, *68*(1), 7-30. doi:10.3322/caac.21442
12
- 13 Sultan, M., Coyle, K. M., Vidovic, D., Thomas, M. L., Gujar, S., & Marcato, P. (2017). Hide-and-
14
15 seek: The interplay between cancer stem cells and the immune system. *Carcinogenesis*, *38*(2),
16
17 107-118.
18
- 19 Tiran, V., Stanzer, S., Heitzer, E., Meilinger, M., Rossmann, C., Lax, S., . . . Balic, M. (2017).
20
21 Genetic profiling of putative breast cancer stem cells from malignant pleural effusions. *Plos*
22
23 *One*, *12*(4), e0175223.
24
25
- 26 Vriens, K., Christen, S., Parik, S., Broekaert, D., Yoshinaga, K., Talebi, A., . . . Fendt, S. (2019).
27
28 Evidence for an alternative fatty acid desaturation pathway increasing cancer plasticity. *Nature*,
29
30 *566*(7744), 403-406. doi:10.1038/s41586-019-0904-1
31
32
- 33 Woo, J. S., Reddy, O. L., Koo, M., Xiong, Y., Li, F., & Xu, H. (2017). Application of
34
35 immunohistochemistry in the diagnosis of pulmonary and pleural neoplasms. *Archives of*
36
37 *Pathology & Laboratory Medicine*, *141*(9), 1195-1213. doi:10.5858/arpa.2016-0550-RA
38
- 39 Yakisich, J. S., Azad, N., Kaushik, V., & Iyer, A. K. V. (2017). Cancer cell plasticity: Rapid
40
41 reversal of chemosensitivity and expression of stemness markers in lung and breast cancer
42
43 tumorspheres. *Journal of Cellular Physiology*, *232*(9), 2280-2286. doi:10.1002/jcp.25725
44
45
- 46 Zhang, F., Duan, S., Tsai, Y., Keng, P. C., Chen, Y., Lee, S. O., & Chen, Y. (2016). Cisplatin
47
48 treatment increases stemness through upregulation of hypoxia-inducible factors by interleukin-
49
50 6 in non-small cell lung cancer. *Cancer Science*, *107*(6), 746-754. doi:10.1111/cas.12937
51
52
53
54
55
56
57
58
59
60

Figure Captions

Figure 1. CytoMatrix: a support to entrap limited amounts of cytological material from MPEs

(a) Representative pictures of the plastic bio-cassette containing CytoMatrix in the closed (left photo) and open (right photo) conformations. (b) The synthetic matrix restraining the biological material either derived from primary cancer cells directly isolated from MPEs and from established primary cell cultures grown in 2D or 3D conditions may be subjected to classical immunocytochemistry (ICC) steps: formalin fixation, paraffin inclusion and microtome cut.

Figure 2. Characterization of primary cells from MPEs using CytoMatrix

(a) CytoMatrix-based ICC staining of Haematoxylin and Eosin, PAN-CK, Vimentin and CD45 on NCI-H460 stable cell line. Original magnification X200. (b) Comparison between staining of different markers obtained from paraffin-IHC and CytoMatrix-based ICC samples of patient BBIRE-T238. Original magnification X200.

Figure 3. CytoMatrix for the study of MPEs-derived CSCs

(a) Representative images of a lung stable cell line, NCI-H460, and BBIRE-T238 derived primary cell line grown in adherent (2D) and in 3D conditions. The pictures are captured on day 4. Original Magnification X100. (b) Gene expression of stemness markers and **SCD1** performed by qRT-PCR analyses on 3D and 2D cultures obtained from NCI-H460 and the primary cell line isolated from malignant pleural effusions of BBIRE-T238 patient. **The bar chart shows the fold change in the mRNA levels in 3D spheroids compared to 2D parental cells (histone H3 was used as housekeeping gene).** Data represent the mean and SD or SEM of at least three independent experiments and are statistically significant if $*p < 0.05$ (Student's t-test). (c) Example of IHC staining of Haematoxylin and Eosin, CK7, PAN-CK, CD45 and TTF-1 performed on lung adenocarcinoma biopsy (upper panels) and of CytoMatrix-based ICC staining of primary cell line derived from BBIRE-T238 patient (middle and bottom panels). The results indicate a similar pattern of expression between biopsy and primary cell cultures. Original magnification X400. (d) SCD1 expression obtained from CytoMatrix-based ICC staining of NCI-H460 and BBIRE-T238 primary cell line in 2D and 3D conditions and from IHC staining of biopsy. Original magnification X200, detail X1000. (e) YAP/TAZ IHC (upper panel) and YAP/TAZ CytoMatrix-based ICC (bottom panel) performed on samples obtained from BBIRE-T238 patient. Original magnification X200, detail X1000. (f) Comparison between YAP/TAZ CytoMatrix-based ICC (panel on the left) and YAP/TAZ

1
2
3 CytoMatrix-based IF (panel on the right) analyses obtained from NCI-H460 grown in 3D
4 conditions. Scale bar 20 μ m.
5
6

7 **Table 1**

8
9 Table shows patient and tumour features. Specific mutation sites are also reported from NGS
10 mutational analysis on both biopsy and primary cell line.
11

12 Abbreviations: CDDP, cisplatin; PEM, pembrolizumab; CNV, copy number variants; VAF, variant
13 allele frequency; N/A, not available.
14
15

16 **Supplementary Figure 1**

17
18 Comparison between staining of different markers obtained from paraffin-IHC and CytoMatrix-
19 based ICC samples of patient BBIRE-T248 (left panels) and BBIRE-T570 (right panels). Original
20 magnification X200.
21
22
23

24 **Supplementary Figure 2**

25
26 (a) Representative images of BBIRE-T248 derived primary cell line grown in adherent (2D) and in
27 3D conditions. The pictures are captured on day 5. Original Magnification X100. (b) Gene
28 expression of stemness markers and SCD1 performed by qRT-PCR analyses on 3D and 2D cultures
29 obtained from the primary cell line isolated from malignant pleural effusions of BBIRE-T248
30 patient. The bar chart shows the fold change in the mRNA levels in 3D spheroids compared to 2D
31 parental cells (β -actin was used as housekeeping gene). Data represent the mean and SD or SEM of
32 at least three independent experiments and are statistically significant if * $p < 0.05$ (Student's t-test).
33 (c) Example of IHC staining of Haematoxylin and Eosin, CK7, PAN-CK, CD45 and TTF-1
34 performed on lung adenocarcinoma biopsy (upper panels) and of CytoMatrix-based ICC staining of
35 primary cell line derived from BBIRE-T248 patient (middle and bottom panels). The results
36 indicate a similar pattern of expression between biopsy and primary cell cultures. Original
37 magnification X400. (d) SCD1 expression obtained from CytoMatrix-based ICC staining of
38 BBIRE-T248 primary cell line in 2D and 3D conditions and from IHC staining of biopsy. Original
39 magnification X200, detail X1000. (e) YAP/TAZ IHC (upper panel) and YAP/TAZ CytoMatrix-
40 based ICC (bottom panel) performed on samples obtained from BBIRE-T248 patient. Original
41 magnification X200, detail X1000.
42
43
44
45
46
47
48
49
50
51
52
53
54
55
56
57
58
59
60

1
2
3
4
5
6
7
8
9
10
11
12
13
14
15
16
17
18
19
20
21
22
23
24
25
26
27
28
29
30
31
32
33
34
35
36
37
38
39
40
41
42
43
44
45
46
47
48
49
50
51
52
53
54
55
56
57
58
59
60

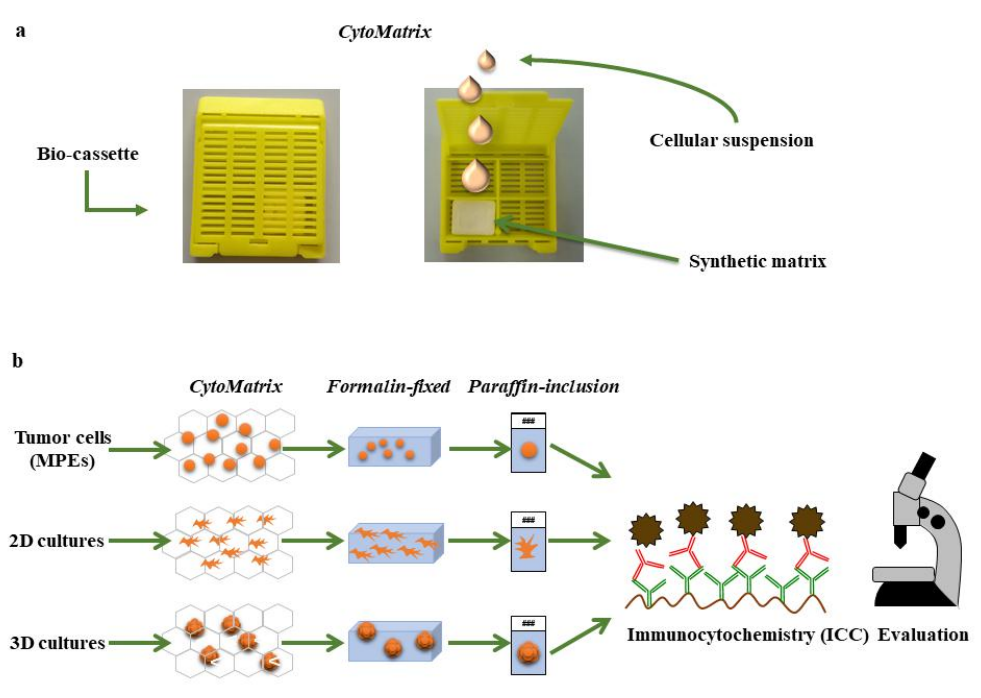


Figure 1. CytoMatrix: a support to entrap limited amounts of cytological material from MPEs

254x190mm (96 x 96 DPI)

1
2
3
4
5
6
7
8
9
10
11
12
13
14
15
16
17
18
19
20
21
22
23
24
25
26
27
28
29
30
31
32
33
34
35
36
37
38
39
40
41
42
43
44
45
46
47
48
49
50
51
52
53
54
55
56
57
58
59
60

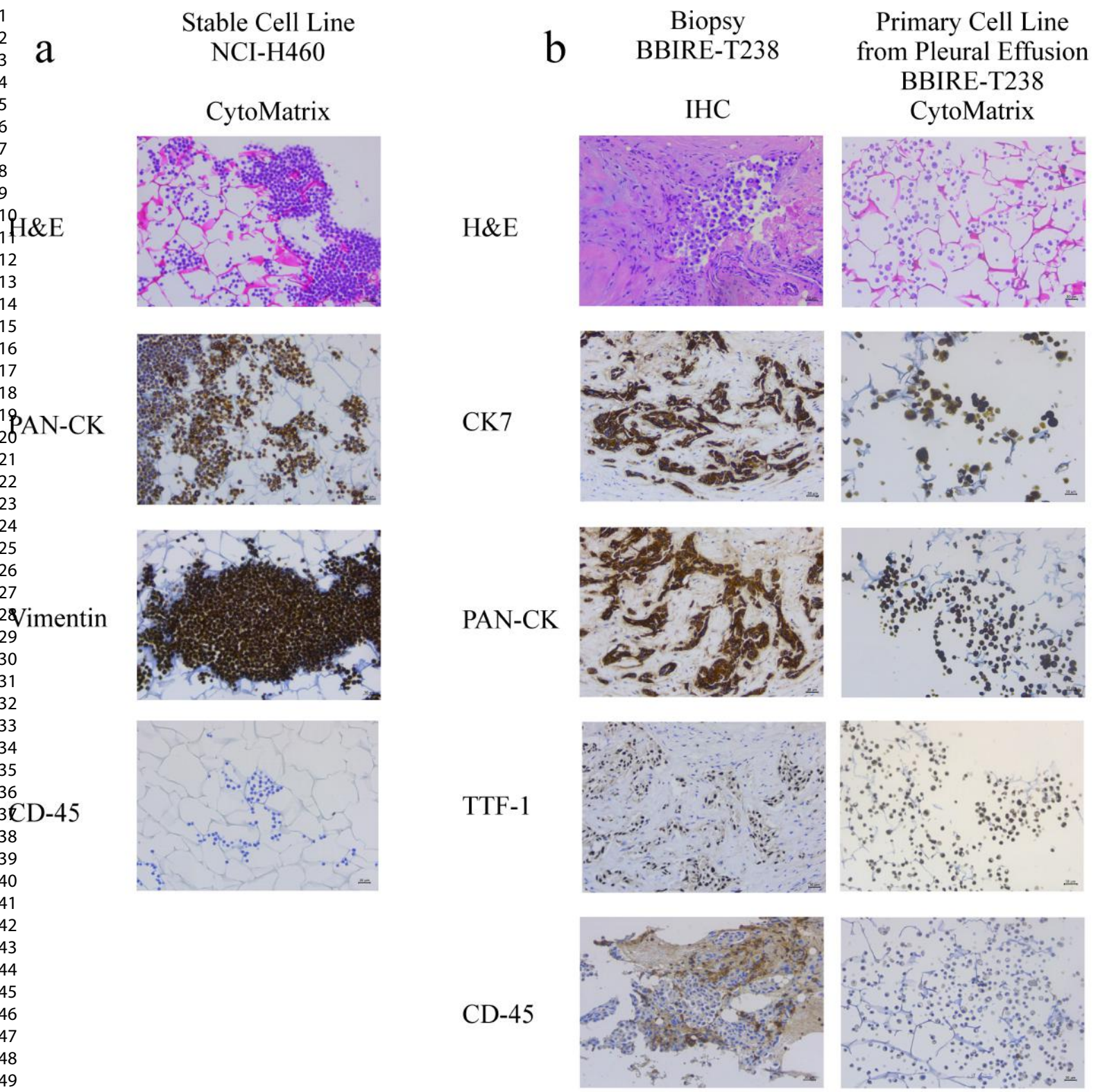


Figure 2

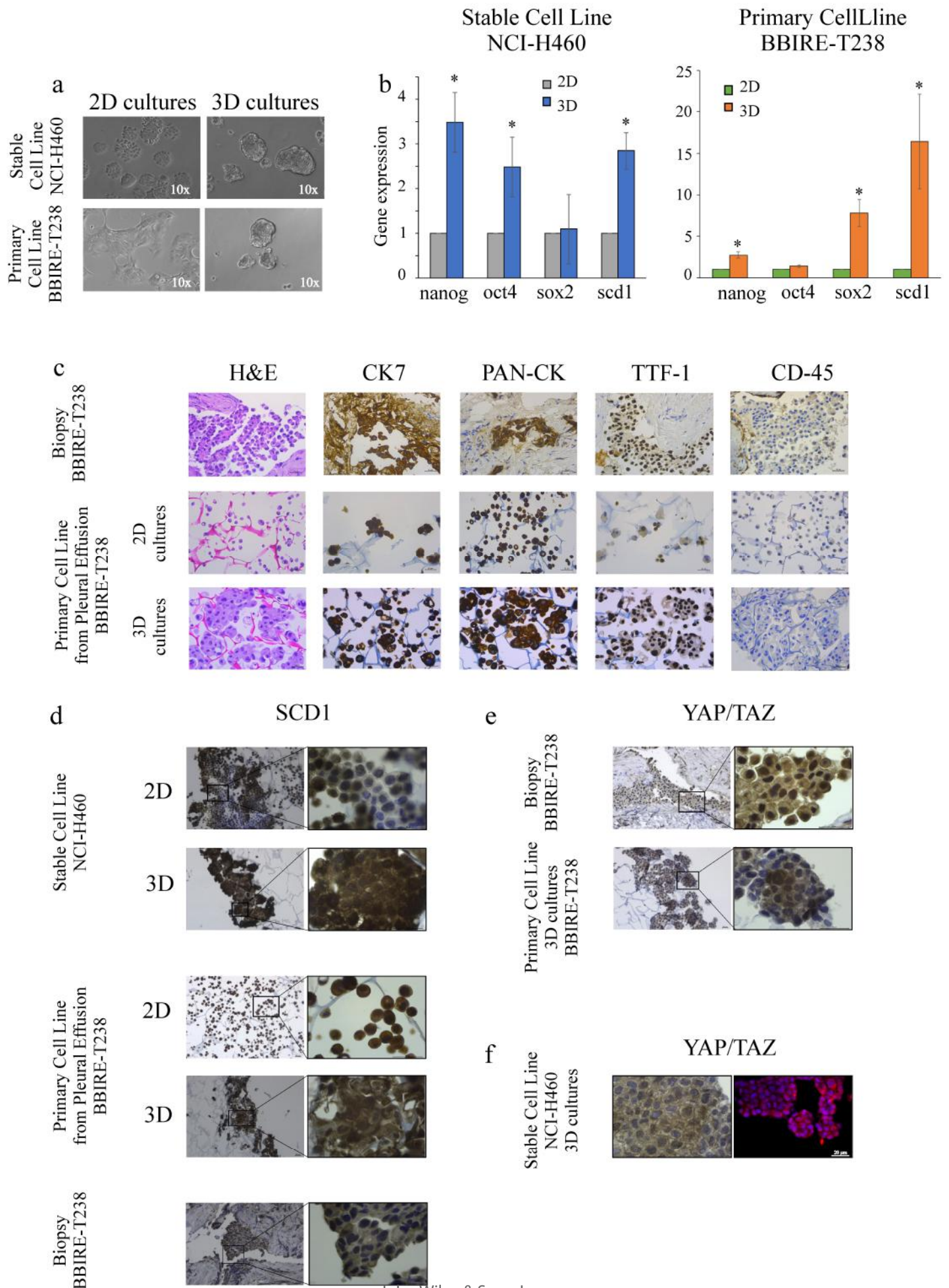


Figure 3

Table 1. Clinicopathological characteristics of three MPE-cases included in the study.

PATIENT_ID	SEX/AGE	SURGERY_LOCATION	DIAGNOSIS	GRADING	DIAGNOSTIC MARKERS	NGS Mutational analysis - Biopsy	NGS Mutational analysis - Primary Cell Line	THERAPY
BIRE-T238	F/60	PLEURAL BIOPSY	ADENOCARCINOMA	3	TTF1+, PDL1+, ALK-, ROS1-	EGFR (p.M766_A767 ins ASV (Level III/II) c.23_2309insCCAGCGTGG, EXON20) VAF: 22%	EGFR (p.M766_A767 ins ASV (Level III/II) c.23_2309insCCAGCGTGG, EXON20) VAF: 43%	CDDP/PEM
BIRE-T248	M/74	PLEURAL BIOPSY	ADENOCARCINOMA	3	TTF1+, PDL1+, ALK-, ROS1-	KRAS (p. G12V (LevelIII/II), c.35G>T, EXON2) VAF:36%	KRAS (p. G12V (LevelIII/II), c.35G>T, EXON2) VAF: 86%	PEM
BIRE-T570	F/46	PLEURAL BIOPSY	ADENOCARCINOMA	3	TTF1+, PDL1+, ALK+, ROS1-	ALK-rearrangement: Fusion EML4- ALK.E17 ins30a20_V8a, gain of function MYC-amplification: CNV 20.4	ALK-rearrangement: Fusion EML4- ALK.E17 ins30a20_V8a, gain of function MYC-amplification: CNV 26.44	N/A

1
2
3
4
5
6
7
8
9
10
11
12
13
14
15
16
17
18
19
20
21
22
23
24
25
26
27
28
29
30
31
32
33
34
35
36
37
38
39
40
41
42
43
44
45
46
47
48
49
50
51
52
53
54
55
56
57
58
59
60

BBIRE-T248

BBIRE-T570

Biopsy

Primary Cell Line
from Pleural Effusion

Biopsy

Primary Cell Line
from Pleural Effusion

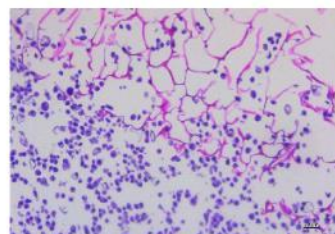
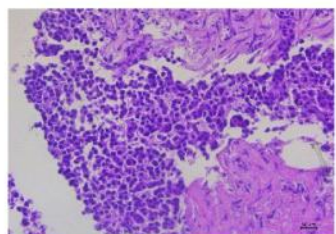
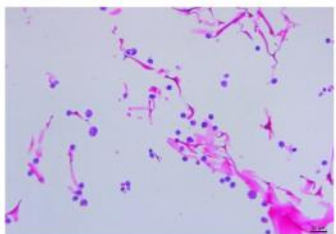
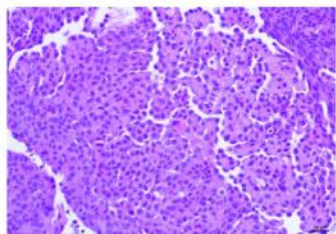
IHC

CytoMatrix

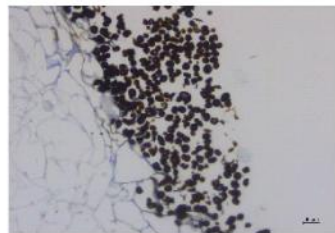
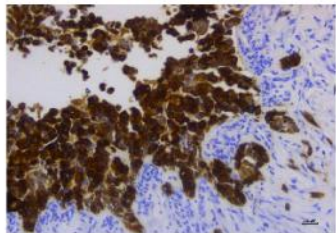
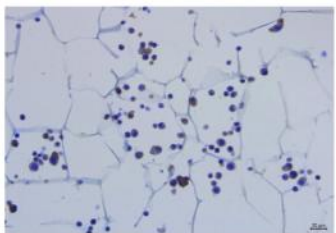
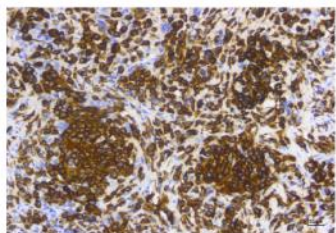
IHC

CytoMatrix

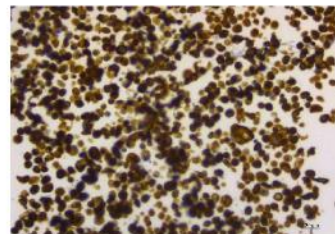
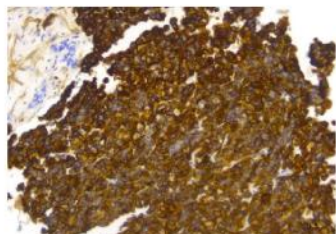
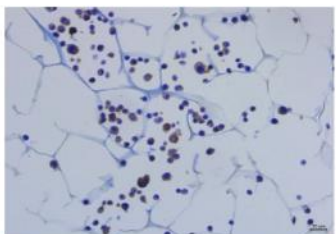
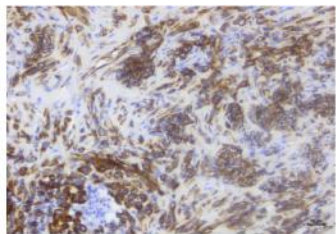
H&E



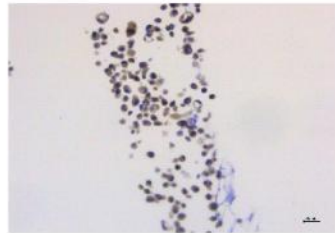
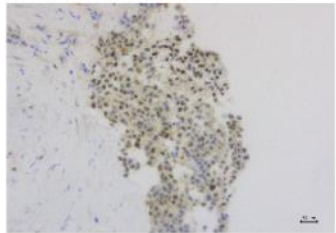
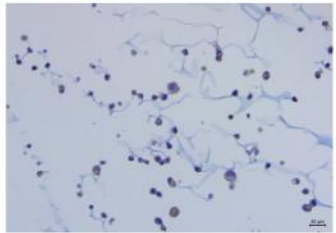
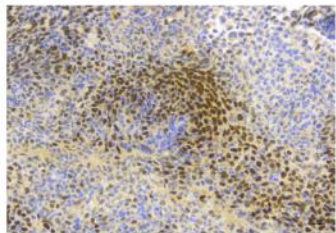
CK7



PAN-CK



TTF-1



CD-45

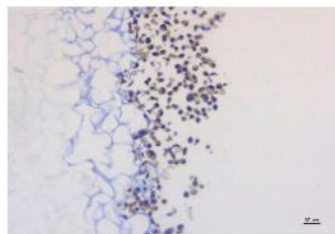
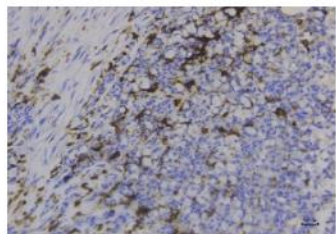
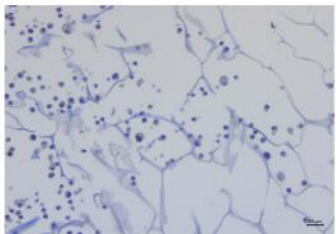
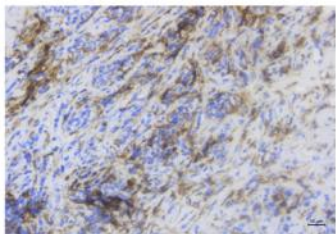
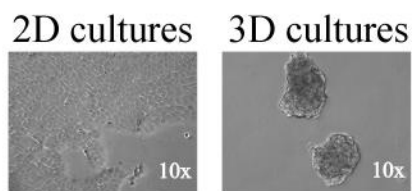


Figure S1

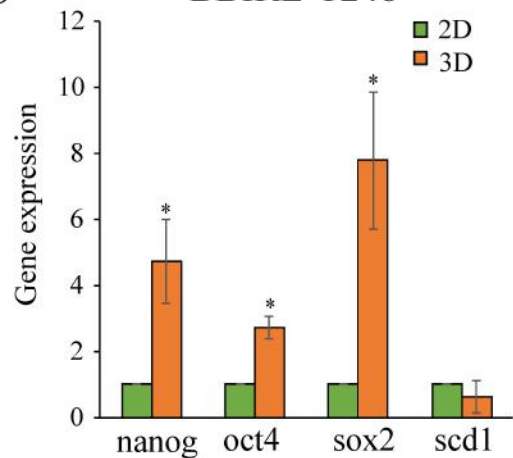
Primary Cell Line
BBIRE-T248

Primary Cell Line
BBIRE-T248

a



b



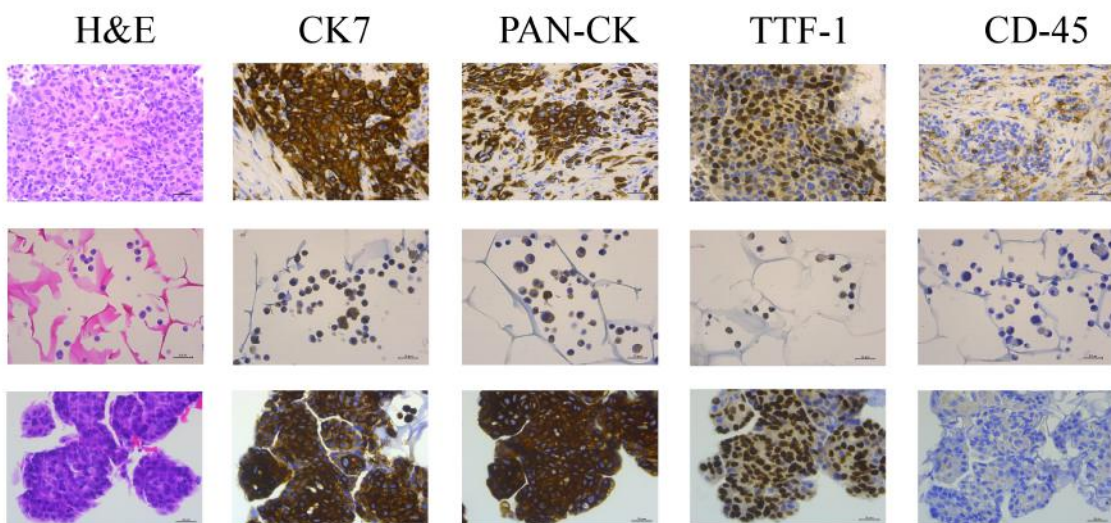
c

Biopsy
BBIRE-T248

Primary Cell Line
from Pleural Effusion
BBIRE-T248

2D
cultures

3D
cultures



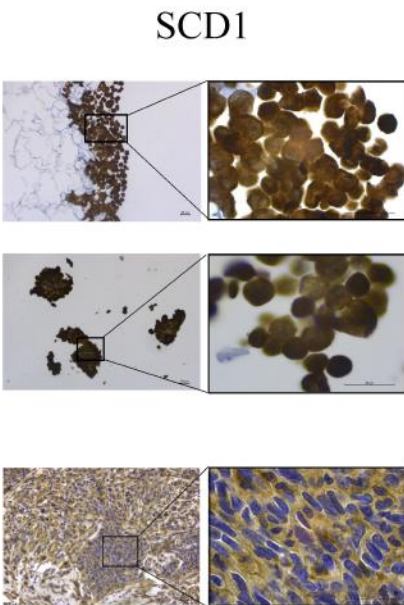
d

Primary Cell Line
from Pleural Effusion
BBIRE-T248

2D

3D

Biopsy
BBIRE-T248



e

Biopsy
BBIRE-T248

Primary Cell Line
3D cultures
BBIRE-T248

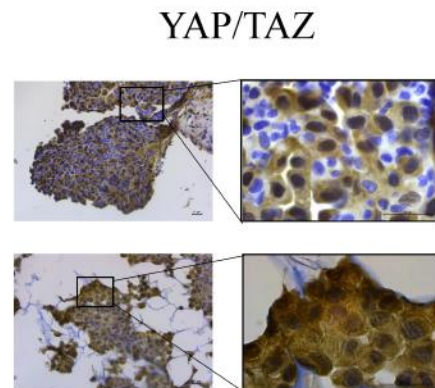


Figure S2

Supplementary Table 1. List of primary antibodies used in IHC/ICC

Antibodies	Source	Catalog number
Anti-Cytokeratin 7	Leica Biosystems	CK7-OVTL-L-CE
Anti-Cytokeratin cocktail AE1/AE2	Leica Biosystems	AE1-AE3-L-LE
Anti-TTF-1	Dako	M3575
Anti-CD45	Dako	M070101
Anti-SCD1 (clone CD.E10)	Abcam	ab19862
Anti-YAP/TAZ	Santa Cruz Biotechnologies	sc-101199

Supplementary Table 2. Primers used for qRT-PCR

Oct4	-Forward 5'- TGGGATATACACAGGCCGATG -3' -Reverse 5'- TCCTCCACCCACTTCTGCAG -3'
Nanog	-Forward 5'- TACCTCAGCCTCCAGCAGATG -3' -Reverse 5'- CCTTCTGCGTCACACCATTG -3'
SCD-1	-Forward 5'- GCAGGACGATATCTCTAGCT -3' -Reverse 5'- GTCTCCAACCTTATCTCCTCCATTC -3'
Sox2	-Forward 5'- CACCCCTGGCATGGCTCTT -3' -Reverse 5'- GAGCTGGCCTCGGAC TTG-3'
Histone H3	-Forward 5'-GACACTAACCTGTGCGCCAT -3' -Reverse 5'-TTTGCTTGACCGTGAGAGA -3'
β -actin	-Forward 5' - GCCGGGACCTGACTGACT-3' -Reverse 5' - TGGTGATGACCTGGCCGT-3'

For Peer Review